Correlations of the Stability, Static Dipole Polarizabilities, and Electronic Properties of Yttrium Clusters

Xi-Bo Li,[†] Hong-Yan Wang,*[,‡] Ran Lv,[§] Wei-Dong Wu,[†] Jiang-Shan Luo,[†] and Yong-Jian Tang*[,†]

Research Center of Laser Fusion, China Academy of Engineering Physics, Mianyang 621900, College of Physical Science and Technology, Southwest Jiaotong University, Chengdu 610031, and Atomic and Molecular Physics Institute, Sichuan University, Chengdu 610065, China

Received: May 12, 2009; Revised Manuscript Received: July 26, 2009

Static dipole polarizabilities for the ground-state geometries of yttrium clusters (Y_n, $n \leq 15$) are investigated by using the numerically finite field method in the framework of density functional theory. The structural size dependence of electronic properties, such as the highest occupied molecular orbital−lowest occupied molecular orbital (HOMO−LUMO) gap, ionization energy, electron affinity, chemical hardness and softness, etc., has been determined for yttrium clusters. The energetic analysis, minimum polarizability principle, and principle of maximum hardness are used to characterize the stability of yttrium clusters. The correlations of stability, static dipole polarizabilities, and electronic properties are analyzed especially. The results show that static polarizability and electronic structure can reflect obviously the stability of yttrium clusters. The static polarizability per atom decreases slowly with an increase in the cluster size and exhibits a local minimum at the magic number cluster. The ratio of the mean static polarizability to the HOMO−LUMO gap has a much lower value for the most stable clusters. The static dipole polarizabilities of yttrium clusters are highly dependent on their electronic properties and are also partly related to their geometrical characteristics. A large HOMO−LUMO gap of an yttrium cluster usually corresponds to a large dipole moment. Strong correlative relationships of the ionization potential, softness, and static dipole polarizability are observed for yttrium clusters.

1. Introduction

The static dipole polarizability is an important quantity in the field of chemistry and physics.[1−4] Polarizability is sensitive to the structural geometry and delocalization of valence electrons of clusters, and is the most important observable for understanding the geometry and electronic properties. Furthermore, polarizability is one of the characteristic properties that can be obtained by experiment, and it can provide information on the bonding and geometrical features of the clusters. The electronic property calculations for Ge, Si, and Au clusters have shown that the polarizability is strongly correlated with the shape of the clusters.[5−8] Calaminici et al.[9] have calculated that the trend of the polarizability per atom of copper clusters, which is similar to the experimental value of sodium clusters, and concluded that the electronic and geometric structures of copper clusters follow a trend similar similar to that for sodium clusters. The interplay between theory and experiment is a powerful tool that serves to identify which cluster is observed in the experiments through the comparison of the calculated polarizabilities with the experimental ones. Therefore, the thorough understanding of the polarizabilities from theoretical calculations is important in cluster science. The polarizabilities of clusters have been extensively studied both theoretically[5−27]and experimentally[28−36] during the past few years.

An interesting issue is concerned with the relationship between static polarizability and ionization potentials. The static electric dipole polarizability describes the distortion of the electron density under the effect of an external static electric field. However, the first ionization potential measures the capability of a cluster to lose one valence electron and thus indirectly reveals how tightly an electron is bound within the nuclear attractive field of the system. An inversely related relationship between ionization potential and polarizability has been first derived and shown to be valid for atomic systems by Dmitrieva and Plindov.[37] Such relationships have been studied for atomic and selected molecular systems with reasonable success.[96,97] In the newly emerging field of metal clusters, such as gold, sodium, and lithium clusters, the relationship between ionization potential and polarizability has also been studied.[26,27] The molecular beam deflection experiment has been used to investigate the electric dipole polarizabilities of aluminum,[28] nickel,[29] niobium,[30,31] noble metals,[32,33] pure and mixed alkali metals,[34−36] etc., but no measurements of static electric polarizabilities have until now been available for yttrium clusters. However, the vertical ionization potentials (VIPs) of Y_n clusters for $n = 2-31$ have been measured by means of photoionization spectroscopy.[38] Therefore, the polarizabilities of Y_n clusters can be predicted by the correlation between the static polarizability and ionization potential through the theoretical methods.

The other interesting issues are the hard−soft acid−base (HSAB) principle and the principle of maximum hardness (PMH), which are concerned with the study of the rationalizing of chemical reactions.[39] It is necessary to explore the possible relationships of these reactivity descriptors with the observable quantities in the experiment. To rationalize the quantitative

* To whom correspondence should be addressed. E-mail: wanghyxx@yahoo.com (H.-Y.W.); tangyongjian@yahoo.cn (Y.-J.T.).
[†] China Academy of Engineering Physics.
[‡] Southwest Jiaotong University.
[§] Sichuan University.

10.1021/jp904420z CCC: $40.75
Published on Web 09/01/2009

definition of the descriptors, several studies have been carried out to show the correlation between the electronic properties and the polarizability.[40−42] The PMH asserts that molecular systems present the highest value of hardness at equilibrium. At this point, many studies show that the PMH may hold even though the chemical potential and external potential vary during the chemical processes.[82−86] In this paper, these quantities in the study of chemical reactivity will be used to characterize yttrium clusters, and it is expected that their relations with stability and static polarizability will be found.

The jellium model has been successfully used to study and indeed provide a reasonable description for many large metallic clusters. However, theoretical predictions for the relatively simple spherical jellium calculations disagree with experiment most significantly for the smaller alkali-metal and aluminum clusters.[4] In addition, for semiconductor and some transition-metal (TM) clusters, bonding and geometrical effects cannot be incorporated into the jellium model. Yang and Jeckson[10] have confirmed that there exists a large difference in polarizability of a small copper cluster between values calculated by the jellium model and observed values. The available approaches which were based on the empirical tight-binding method also exhibit rather strong diversity.[11,12] Torrens[13,14] has calculated the molecular dipole−dipole polarizabilities of Sc_n, C_n, and endohedral $Sc_n@C_m$ clusters by using a polarization model based on interacting dipoles. He has pointed out that a calibration of the ab initio calculations is needed as a primary standard to reduce the large differences between their POLAR and PAPID programs. These possibly come from an uncertainty in the correct ground-state structure with the atomic structures obtained by using an empirical potential. It would be very useful to obtain cluster structures at a more reliable level of theory, such as density functional theory (DFT). Previous works have shown that density functional methods are able to yield reliable values for the static dipole polarizability of atoms,[15−17] molecules, and clusters.[5−10,18−27] DFT methods have made substantial progress, and they are one of the most effective tools for the computation of structure and electronic properties of molecules and clusters in the ground state. The two most popular first-principle calculations of static and dynamical polarizabilities in linear response are the time-dependent local-density approximation (TDLDA) and finite field (FF) method. Some quantum chemistry techniques such as coupled cluster and configuration interaction methods are also used to study the static and dynamical polarizabilities.

For yttrium clusters, most studies are limited to the dimer and trimer.[43−47] Recently, the structural, electronic, and magnetic properties of yttrium clusters up to 17 atoms have been obtained by density functional DMol calculations.[48] Dai et al.[49] have studied the VIPs of Y_n ($n = 1-4$) clusters using complete active space multiconfiguration, and Durakiewicz et al.[50] have calculated the ionization potential of small yttrium clusters by using the conducting spherical droplet (CSD) model in which the quantum effects were not included to explain the dependence on cluster size. Our group also has calculated the geometrical structures and ionization potential for Y_n ($n = 2-8$) clusters by using DFT.[51] However, the static dipole polarizabilities of yttrium clusters, related strongly to the measurable experimental results, have not been studied up to now. No systematic DFT investigation on the correlations of the stability, the static dipole polarizability, and the electronic properties of yttrium clusters has been conducted thus far. Thus, our previous DFT studies[52,53] on the static polarizabilities of noble-metal clusters are extended to yttrium clusters. The static dipole polarizabilities of yttrium clusters (Y_n, $n \leq 15$) are investigated by using the numerical FF method in the framework of DFT. The size dependence of several reactivity descriptors, such as the highest occupied molecular orbital−lowest occupied molecular orbital (HOMO−LUMO) gap, ionization potential, hardness, and softness, is explored, and the interrelationships of the relative stability, static dipole polarizabilities, and electronic properties are investigated in this paper.

2. Computational Details

2.1. DFT Method. Electronic exchange and correlation effects are well-known to play a primary role in determining molecular polarizabilities.[54] In the calculations of molecular polarizabilities and hyperpolarizabilities, the DFT method provides significant improvement compared to the Hartree−Fock method and less computer time than the ab initio methods,[55,56] and for metallic clusters where the HOMO−LUMO gap is very small and single-reference methods fail, DFT seems to be the appropriate choice. The suitable DFT method needs to be determined first because the geometries, electronic properties, and polarizabilities of molecules or clusters are also quite sensitive to the exchange-correlation functional used in the DFT method. Our previous study showed that the BP86 functional is the most suitable DFT method for some TM clusters[57] in which the Perdew 86 (P86) correlation functional[58] and pure DFT exchange functional of 1988(B)[59] are included.

The explicit treatment of all electrons in a heavy TM cluster which has a large number of atoms and electrons constitutes a demanding computational task. One of the best ways to surmount this difficulty is to make use of electron core potentials (ECPs), which are also known as pseudopotentials.[60] Many previous studies have confirmed that ECP treatment can provide a feasible and accurate approach for electronic properties.[61] Jansik et al. employed a large-core ECP for Si in the study of the static polarizability of silicon clusters.[62] Their results showed modern ECPs can provide excellent approximations to all electron values in all cases; the error for polarizability is on the order of 1%. The pseudopotentials have been extensively used to explore the polarizability for many TM clusters, such as Cu_n,[21] Ag_n,[24,25] Au_n,[7,8,26] Ge_n,[5,63] Zn_n,[18] etc. Finally we also notice that static polarizabilities of gold clusters were studied by Idrobo et al.,[8] in which the values obtained by using the scalar-relativistic pseudopotential method are in very good agreement (only 3% higher on average) with the results of our previous study with the ECPs and corresponding valence basis set for gold clusters.[52] In the present paper, the CEP-121G ECP basis sets[64] including the relativistic effect are chosen to eliminate some atomic core electrons and reduce the cost of computations for the polarizability of yttrium clusters, in which the dependence of spin−orbit effects was averaged out, and the valence electrons of the Y atom are $4s^24p^64d^15s^2$.

To test the reliability of our calculation, the spectroscopic constant properties of the Y_2 dimer and Y_3 trimer are calculated and compared with the previous experimental and theoretical studies. The detailed analysis also can be found from our recent work,[57] in which the results obtained by using several different exchange-correlation functionals combined with the different basis sets are compared. At the BP86/CEP-121G level, the quintet state ($^5\Sigma_u$) is the ground state in accord with the electron spin resonance (ESR) experimental result[44] and the method of CASSCF-CI calculation.[65,66] The computed dissociation energy of 1.54 eV for Y_2 is well reproduced in comparison with the measured value of 1.62 ± 0.22 eV.[44,67] The obtained vibrational frequencies of 180.6 cm^{-1} also agree with the experimental value

of 185 or 184.4 cm^{-1}.[44,68] Until now, no experimental data have been available for the equilibrium bond length of Y_2. However, our calculated value (2.946 Å) compares favorably with the result obtained by using Pauling's rule, which is 2.74 Å.[69] For the Y_3 trimer, our results show that the ground state is an isosceles triangle at a spin double state ($^2A_1'$). The energies of linear structures are much higher than those of triangular structures, and the energy of an equilateral triangle (C_{3v}) is 0.07 eV higher than that of an isosceles triangle (C_{2v}), which is in agreement with the experimental study of ESR[43] and previous theoretical studies.[45,46,48] Comparisons between our calculated results of Y_2 and Y_3 and measurements as well as the results of previous theoretical calculations show that DFT is adequate for calculating their bond lengths and relative energetic and electronic properties. Therefore, it is expected that the selected BP86/CEP-121G DFT level can be reliably used to predict the properties for the larger yttrium clusters.

The total energy of yttrium clusters has been calculated, and the geometrical structure with the lowest energy is chosen as the ground-state geometry. When the cluster has less than six atoms, the default SCF convergence of 10^{-8} is used. For the larger clusters ($n \geq 6$), the computation cannot converge except to a 10^{-6} tolerance. The thresholds for convergence are 0.00045 and 0.0003 au for the maximum force and root-mean-square force, respectively. All of the calculations are performed in spin-unrestricted conditions for all allowable spin multiplicities. The set of starting configurations chosen is extensive enough to ensure sufficiently thorough exploration of the cluster potential energy surfaces including all structures found in our earlier studies[57] and reasonable geometries of TM in other previous works. With increasing cluster size, such calculations become computer time demanding and the search for stable structures of larger clusters becomes more difficult because of the increasing number of possible isomers. Therefore, the strategy of adding or capping smaller clusters is used.[52] The key point of the calculations is fixing the starting geometry of the cluster, which could converge during the calculation to a local minimum or to the global energy minimum structure. Many different cluster structures have been examined for their stability and relative energies, and all isomers are confirmed to be the genuine minima by the harmonic vibrational frequency calculation.

2.2. Finite Field Treatment. The static response properties of a molecule can be defined in two different ways. The field-dependent energy $E(\mathbf{F})$ can be expanded in a series:

$$E(\mathbf{F}) = E(0) - \sum_i \mu_i F_i - \frac{1}{2}\sum_{ij} \alpha_{ij} F_i F_j - \ldots\ldots \quad (1)$$

where $E(0)$ is the total energy of the molecular system in the absence of the electric field, the quantities F_i are components of the applied field in different directions ($i, j = x, y, z$), and μ_i and α_{ij} are components of the static dipole moment and polarizability tensor, respectively.

Alternatively, the static response properties of a molecule can be defined by expanding the field-dependent dipole moment, calculated from the field-induced charge distribution, as a series of the external electric field:

$$\mu_i(F) = -\frac{\partial E(\mathbf{F})}{\partial F_i} = \mu_i(0) + \sum_j \alpha_{ij} F_j + \ldots\ldots \quad (2)$$

The equivalence of these two definitions for field-independent basis sets are in accord with the Hellmann−Feynman theorem.[98,99] In our density functional calculation, the dipole moment expansion is used and the polarizability is defined by

$$\alpha_{ij} = \frac{\partial \mu_i(\mathbf{F})}{\partial F_j} = -\frac{\partial^2 E(\mathbf{F})}{\partial F_i\, \partial F_j} \qquad i, j = (x, y, z) \quad (3)$$

Using the finite difference expressions for the first and second derivatives, the diagonal elements of the polarizability tensor α_{ii} can be foundd from the dipole moment $\mu_i(\mathbf{F})$ or from the total energy $E(\mathbf{F})$ at $\mathbf{F} = 0$ and $\mathbf{F} = \pm\delta F_i$ applied along the ith axis.

In the present work, the external field is applied along the x, y, and z axes with a magnitude of 0.005 au and a tighter self-consistent field (SCF) convergence of 10^{-8} hartree is adopted as a criterion. These values have been found to yield well-converged results for the polarizability. The measured data in experiments are usually the mean polarizabilities ($\langle\alpha\rangle$), and it is sufficient to compute only the diagonal components α_{ii} of the polarizability tensor, which can be obtained by the trace of the polarizability tensor to be

$$\langle\alpha\rangle = \frac{1}{3}\,\mathrm{tr}(\alpha_{ij}) = \frac{1}{3}(\alpha_{xx} + \alpha_{yy} + \alpha_{zz}) \quad (4)$$

It was Noel Hush that pioneered finite field methods in the early 1970s.[100−103] The finite field method used in our work was developed by Kurtz et al.[70] for semiempirical methods. Because of rotational invariance of the trace of the polarizability tensor, this value does not depend on the choice of the coordinate system. The finite field approach[70] implemented within the Gaussian 03 package[71] is used to calculate dipole moment and static electric polarizability components at the BP86/CEP-121G level. In the DFT framework, BP86 functionals combined with CEP-121G basis sets can give a good description of the bonding as well as the geometrical and electronic features of TM clusters. Thus, our method is expected to describe the yttrium cluster polarizabilities well at a level of acceptable computational precision and time.

2.3. Reactivity Descriptors. In DFT, the molecular chemical potential (μ) and global hardness (η) for the N-electron system with total energy E and external potential $v(r)$ are defined as the following first and second derivatives of the energy with respect to N:[72−75]

$$\mu = \left(\frac{\partial E}{\partial N}\right)_{v(r)} \quad (5)$$

$$\eta = \frac{1}{2}\left(\frac{\partial^2 E}{\partial N^2}\right)_{v(r)} = \frac{1}{2}\left(\frac{\partial \mu}{\partial N}\right)_{v(r)} \quad (6)$$

The global hardness has been an indicator of the overall stability of the system, and its inverse defines the global softness as

$$S = 1/2\eta \quad (7)$$

It has been customary to employ a finite difference approximation to the derivatives, using the energies of N-, $(N + 1)$-, and $(N - 1)$-electron systems; thus, μ, η, and S are calculated through the following approximate equations:[72]

$$\mu \approx -(\mathrm{IP} + \mathrm{EA})/2 \quad (8)$$

$$\eta \approx (\mathrm{IP} - \mathrm{EA})/2 \quad (9)$$

$$S \approx 1/(\mathrm{IP} - \mathrm{EA}) \quad (10)$$

where IP and EA are the first vertical ionization energy and electron affinity of the chemical species, respectively.

In the present paper, we expect to provide a method to understand and if possible to characterize yttrium clusters by reactivity descriptors which have already been successfully used in rationalizing different kinds of molecular structures and chemical reactions.[76−79] DFT has provided the basis for rigorous mathematical definitions of reactivity descriptors,[39,74,80,81] such as the chemical potential (μ), chemical hardness (η), and chemical softness (S), etc. The chemical potential μ characterizes the escape tendency of electrons from equilibrium, the hardness η can be seen as a resistance to charge transfer, and the softness S has been qualitatively related to the polarizability of the system.

3. Results and Discussion

3.1. Equilibrium Geometry and Relative Stability. The equilibrium geometries are obtained at the BP86/CEP-121G level of DFT for Y_n ($n \leq 15$) clusters. On the basis of the optimized geometries of the lowest energy structure, the static polarizability of the cluster is calculated by using the FF method in the framework of DFT. It is important to identify the correct ground-state structure for the yttrium cluster because the static polarizability is a ground-state property which is close to its geometrical characteristic. To avoid trapping at local minima of the potential energy surface, many different initial structures are used, but only the results from the global minimum are presented and are used to calculate polarizabilities by the FF method. The optimized structures of the ground state of these minima, composed of 3−15 atoms, are illustrated in Figure 1. The symmetry and average bond length of Y_n ($n \leq 15$) clusters are listed in Table 1. For all Y_n ($n > 3$) clusters, both the lowest energy structures and their isomers which are not depicted here are all closed compact arrangements.

To analyze the stability and the size-dependent physical properties of Y_n clusters, the total binding energy (E_b), binding energy per atom (E_b/n), fragmentation energy [$D(n, n-1)$], and second-order difference in the total cluster energy [$\Delta_2 E(n)$] are calculated. Figure 2 illuminates the E_b/n, $D(n, n-1)$, and $\Delta_2 E(n)$ values of the ground state, which generally increase with increasing cluster size. The values of the magic numbers (n) for local stability maxima are found to be 4, 7, 11, and 13, implying that these clusters are obviously more stable than their neighboring clusters. The result also shows that the maximum magic number for the relative stability is $n = 7$ and 13 among the Y_n ($n \leq 15$) clusters. The results for ground-state structures except for the Y_{14} cluster and the relative stability are fairly close to those presented by recent studies of Y_n clusters using DFT within the DMol3 package.[48,87] The ground-state structure of the Y_{14} cluster is obtained by adding one yttrium atom to the structure of the Y_{13} cluster, which is based on icosahedral packing, and it is the third lowest energy isomer by Yuan et al. and is only 0.03 eV/atom higher than the ground-state structure.[48] The high stability of clusters may be partially attributed to the high-symmetry geometries and compact atomic arrangements of the clusters.[48] The behavior of the variations is different from that of alkali- and noble-metal clusters, which exhibit characteristic shell oscillations with respect to the cluster size. Thus, the results indicate that the geometrical dense gather other than the electronic shell jellium model, which can provide a reasonable description for Y_n ($n \leq 15$) clusters.

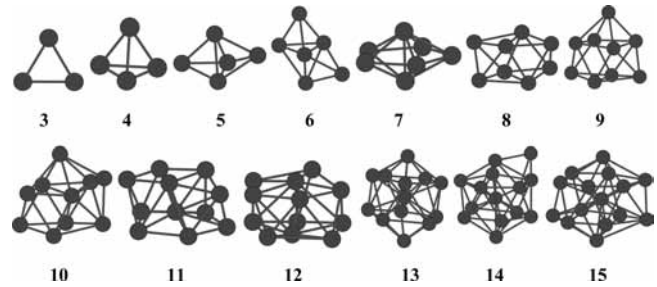

Figure 1. Calculated ground-state geometries of Y_n ($n = 3-15$) clusters.

3.2. Correlations of the Stability and Some Reactivity Descriptors. ***3.2.1. Static Dipole Polarizability.*** Our calculated static dipole polarizability for atomic Y is 140.939 au (20.983 Å^3), which is consistent with the result by Chu et al..[88] They gave a value of 138.97 au for the polarizability of the Y atom by using a linear response TDDFT method. Unfortunately, it is impossible for us to find any other theoretical and experimental polarizability for yttrium clusters. The bulk limit for the polarizability, estimated from the Clausius−Mossotti relation, $\alpha = (3(\varepsilon - 1)\nu)/(4\pi(\varepsilon + 2))$, in which ν is an elementary volume per atom in the crystalline state and ε is the bulk relative dielectric constant. For metals, ε approaches infinity and the dependence of α on ε disappears. In this work, the ν value used for Y is 19.8 Å^3/atom and the polarizability α of the bulk yttrium is calculated to be 4.727 Å^3/atom. The present mean static polarizabilities of Y_n ($n \leq 15$) clusters are all larger than the bulk value. This illuminates the fact that the clusters are all more polarizable than the bulk counterparts. The high polarizability of small clusters is attributed to dangling bonds in the cluster surface. For the alkali-metal and some semiconductor clusters, the polarizability also has been shown to exceed significantly the bulk limit and tends to decrease with increasing cluster size.[4,12]

A graph of the polarizabilities computed for the most stable structures of the clusters is depicted in Figure 3. The static polarizability per atom decreases slowly with an increase of the cluster size, accompanied by some local oscillations. By increasing the cluster size, the polarizabilities of Y_n ($n \leq 15$) clusters exhibit local minima for $n = 4$, 7, 9, 11, and 13, which all have small polarizabilities compared with their neighbors in cluster size. The minimum polarizability principle (MPP) states that any system evolves naturally toward a state of minimum polarizability.[89−91] By applying the MPP to chemical reactivity, those clusters with the local minimum polarizability are more stable than the neighboring clusters. This is consistent with the above discussion on the stability by energetic analysis for yttrium clusters. Thus, polarizability is associated with stability for yttrium clusters.

3.2.2. Chemical Hardness. The chemical hardness values are calculated through eq 9 by using the VIP and EA values. The values of EA are listed in Table 1, which are determined to undermine the corresponding electrophilicity value by DFT method. Chemical hardness has been established as an electronic quantity which may be used to characterize the relative stability of molecules and aggregates in many cases by the PMH. Assuming that the PMH holds in these systems, the hardness is expected to present a behavior with a local maximum at the number of magic clusters. Figure 4 plots the chemical hardness

TABLE 1: Calculations of the Symmetry (Sym), Average Bond Length (R), Binding Energy (E_b), HOMO−LUMO Energy Gap (E_{gap}), Static Dipole Moment (μ), Mean Static Polarizability per Atom ($\langle\alpha\rangle/n$), Vertical Ionization Energy (VIP), and Electron Affinity (EA) of the Lowest Energy Structures for Y_n ($n = 2-15$) Clusters

n	Sym	R(Å)	E_b(eV)	E_{gap} (eV)	μ (D)	$\langle\alpha\rangle/n$ (Å^3)	VIP (eV)	EA (eV)
2	$D_{\infty h}$	2.951	1.537	0.470	0.000	20.995	4.83	0.23
3	D_{3h}	3.179	3.987	0.763	0.000	18.013	4.89	0.57
4	T_d	3.245	7.012	0.368	0.131	14.913	4.68	0.45
5	C_{3v}	3.269	9.794	0.413	0.371	16.269	4.32	0.36
6	C_{2v}	3.276	12.557	0.303	0.209	15.489	4.30	0.48
7	D_{5h}	3.302	15.809	0.451	0.540	14.129	4.52	0.42
8	C_{2v}	3.317	18.465	0.383	0.302	14.542	4.12	0.75
9	C_{2v}	3.339	21.249	0.192	0.241	13.986	4.27	0.64
10	C_{3v}	3.355	24.052	0.222	0.108	14.543	4.23	0.87
11	C_s	3.475	27.134	0.274	0.331	13.573	4.12	0.83
12	C_1	3.487	30.133	0.144	0.316	16.488	3.98	0.72
13	C_{5v}	3.453	33.561	0.349	0.435	13.917	4.26	0.86
14	C_s	3.488	36.467	0.315	0.238	15.734	4.11	1.07
15	C_1	3.491	39.495	0.199	0.228	15.516	4.17	1.28

(η) for the lowest energy Y_n ($n \leq 15$) clusters with increasing cluster size. The magic clusters for Y_7, Y_9, and Y_{13} present higher values of hardness than their neighboring clusters. This also means that the stable magic number clusters are harder than their neighboring systems, which confirms that the stability of yttrium clusters is a manifestation of the PMH. Thus, the maximum hardness is also associated with the stability for yttrium clusters.

3.2.3. Ratio of the Mean Static Polarizability to the HOMO−LUMO Gap. A simple correlation is observed between the polarizability and HOMO−LUMO gap for some clusters with special cluster sizes. Figure 5 plots the ratio of the mean static polarizability to the HOMO−LUMO gap as a function of the cluster size. The much lower ratios of the clusters with magic number $n = 7$, 11, and 13 come from the negative correlation between the polarizability and HOMO−LUMO gap. For example, in Table 1, the HOMO−LUMO gap of Y_7 is bigger than that of Y_8, while the polarizability of Y_7 is smaller than that of Y_8. The same relationship is also found for the Y_{11} and Y_{12} clusters. Thus, Y_{11} has a larger HOMO−LUMO gap than Y_{12}, while the polarizability of Y_{11} is smaller than that of Y_{12}. Then the ratio of the mean static polarizability to the HOMO−LUMO gap is a self-defined parameter, i.e., a reactivity descriptor, which can reflect the relative stability for yttrium clusters.

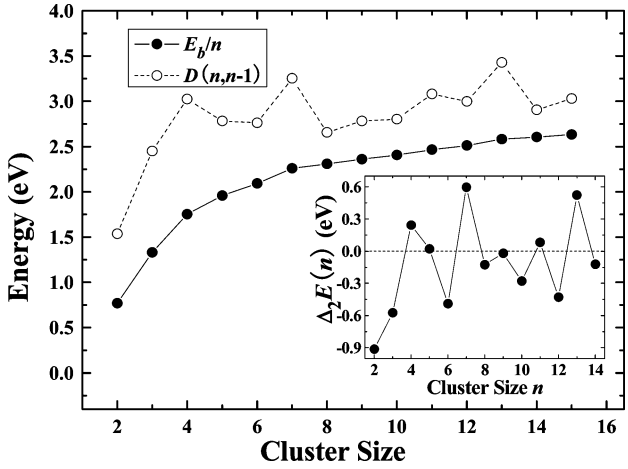

Figure 2. Binding energy per atom (E_b/n), fragmentation energy [$D(n, n-1)$], and second-order difference in the total cluster energy [$\Delta_2E(n)$] of the lowest energy Y_n ($n = 2-15$) clusters.

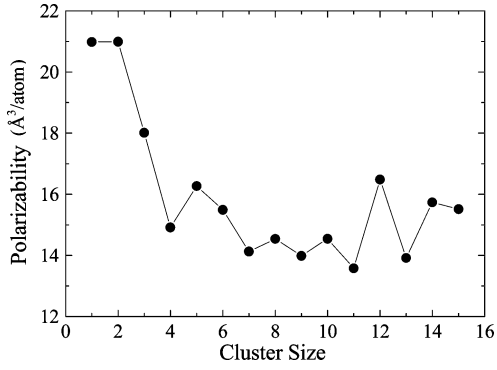

Figure 3. Static polarizability per atom of the lowest energy Y_n ($n \leq 15$) clusters as a function of the cluster size.

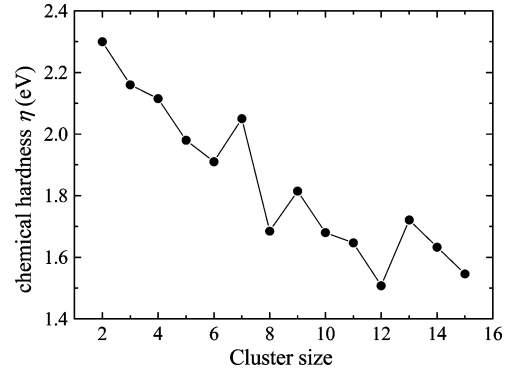

Figure 4. Chemical hardness (η) for the lowest energy structures as a function of the cluster size.

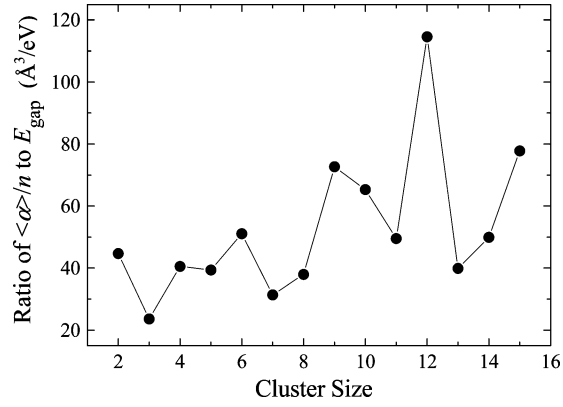

Figure 5. Ratio of the polarizability per atom ($\langle\alpha\rangle/n$) to the HOMO−LUMO gap (E_{gap}) vs the cluster size.

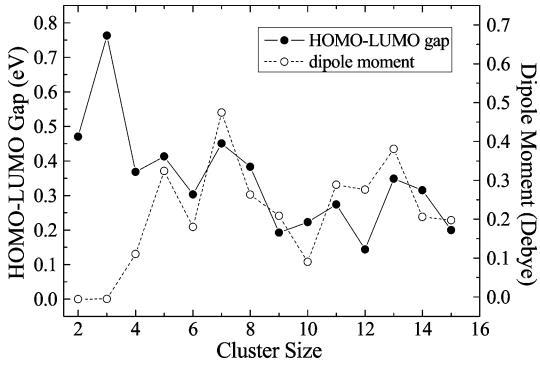

Figure 6. HOMO−LUMO gaps and dipole moments of Y_n ($n \leq 15$) clusters, each as a function of the cluster size.

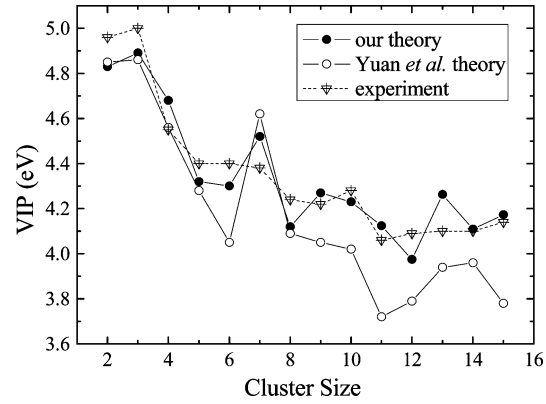

Figure 7. VIPs of Y_n ($n \leq 15$) clusters vs the cluster size.

3.3. Correlations of the Static Dipole Polarizability and Some Electronic Properties. ***3.3.1. HOMO−LUMO Gap.*** The dipole moments may be influenced by the temperature effect.[10] The dipole moments calculated are generally very small in the optimized structures obtained by the FF method in which a temperature of 0 K has been assumed. The dipole moments are so low that the obvious relationship between the dipole moment and the symmetry as the cluster size increases cannot be observed. For some semiconductor and TM clusters, higher symmetry often leads to a relatively low dipole moment for different geometrical structures.[5,26,63] The dipole moments are found from our calculations to be closely related to the electronic properties. The dipole moments are plotted together with the HOMO−LUMO gap as a function of the cluster size in Figure 6, in which for all of the Y_n ($n \leq 15$) clusters the HOMO−LUMO gap and dipole moment follow the same evolutionary trend as the cluster size increases. Therefore, useful information can be obtained from the correlativity of the HOMO−LUMO gap and the dipole moment.

The electronic properties such as the HOMO−LUMO energy gap usually have some influence on the static dipole polarizability. For example, simple perturbation theory suggests that polarizability should be inversely correlated to the HOMO−LUMO gap.[12] In perturbation theory, polarizability is expressed as a sum of contributions from all excited states.[92] A clear correlation between the polarizability and the HOMO−LUMO gap holds if the dominant excited state is mainly described by the HOMO-to-LUMO transition.[26] This also can be easily rationalized using the two-level model:[93]

$$\alpha \approx \frac{\mu_t^2}{\Delta_t} \tag{11}$$

where α is the polarizability, μ_t^2 is the transition dipole moment from the ground state to the first dipole-allowed excited state, and Δ_t is the corresponding transition energy. Approximately, Δ_t can be replaced with the HOMO−LUMO energy gap. From this model, the polarizability increases with decreasing HOMO−LUMO gap. In the present study, however, such a correlation is not observed obviously for Y_n clusters. As shown in Table 1, we can see that some clusters with a small (large) HOMO−LUMO gap also easily tend to have small (large) polarizability. For example, the HOMO−LUMO gap of Y_8 is larger than that of Y_9, while the polarizability of Y_8 is also larger than that of Y_9. Similar results have also been reported for copper and gold clusters.[26] However, as the above discussion indicates and as shown in Figure 5, the most stable clusters with a magic number have much lower ratios, which can be understood by the above model, in which polarizability is inversely correlated to the HOMO−LUMO gap.

However, the above discussion, which describes polarizability as only partially arising from the HOMO-to-LUMO transition, makes unclear the correlation between the HOMO−LUMO gap and the polarizability for Y_n clusters. This may be attributed to another influencing factor, which is their slight structural difference, although the observed structures of Y_n ($n > 3$) clusters are all closed compact arrangements. The polarizability per atom in a cluster is a quantity related to its volume per atom. The more compact structures have relatively few and short bonds, which leads to a more compact cluster and tighter bonding of the valence electrons. For example, the lowest energy structure of Y_7 is the pentagonal bipyramid (Figure 1), which is a more compact geometry than the triangular dodecahedral (bisdisphenoid) structure of Y_8. As a result, the polarizability of Y_7 is smaller than that of Y_8. Thus, a smaller volume is obtained in the more compact structure, which leads to smaller polarizability. Then the polarizability of Y_n clusters is also related to the geometrical characteristics except for the electronic properties. In addition, our optimized isomers of Y_n ($n > 3$) clusters do not appear to be planar and noncompact structures; except for the main series structure of the lowest energy clusters, another integral series of the prolate configuration for Ge clusters[5] and the hollow cage for Au clusters[26] were obtained. In this paper, our results for the optimized isomers are all compact arrangements for Y_n ($n > 3$) clusters. Therefore, at present we cannot further discuss the effects of geometrical arrangements on the polarizability of Y_n clusters.

3.3.2. Ionization Potential. The ionization potential is a quantity indicating the capability of a cluster to lose one valence electron. The variation of the ionization potentials with respect to the size evolution of Y_n clusters is examined. The VIP value at the BP86/CEP-121G level obtained by using a more accurate DFT method is listed in Table 1, and Figure 7 represents the calculated VIP value as a function of the Y_n ($n \leq 15$) clusters size and also shows the theoretical calculation results by Yuan et al.[48] using the GGA method and experimental measurements by Knickelbein et al.[38] As shown in Figure 7, the calculated trend of the size dependence is in good agreement with the earlier computational studies, and our values are closer to the experimental measurements than the results of Yuan et al. The discrepancies between the experiment and theory for TM clusters have been explained and attributed to several possible causes,[48] such as the calculated theory, geometrical structure, condition of the experimental measurement, etc. However, we believe that it is very significant for reference of measurement to compare the different theoretical methods.

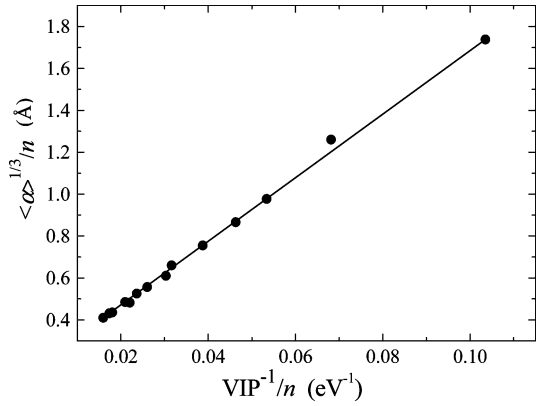

Figure 8. Relationship between the polarizabilities ($\langle\alpha\rangle^{1/3}/n$) and the inverse of the vertical ionization potential (VIP^{-1}/n) of the lowest energy structure clusters.

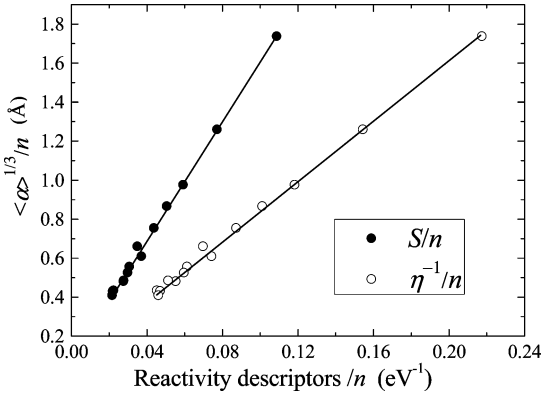

Figure 9. Relationships between the polarizability and chemical softness and hardness.

The static polarizability is a measurement of the distortion of the electron density under an external static electric field, and the higher ionization energy leads to a stronger binding of the valence electron. It is also known that an inverse relationship between ionization potential and polarizability is obtained for neutral atomic systems. In recent work, the ionization energy is found to correlate inversely with the static polarizability for gold, sodium, and lithium clusters.[26,27] As displayed in Figure 8, the polarizability of Y_n clusters is clearly related to the VIP. The cube root of the polarizability per atom ($\langle\alpha\rangle^{1/3}/n$) is directly proportional to the inverse of the vertical ionization energy per atom (VIP^{-1}/n) for yttrium clusters. A strong correlation is observed in which $\langle\alpha\rangle^{1/3}/n$ increases monotonically and linearly with increasing VIP^{-1}/n. The linear correlation is approximately a linear equation with a slope of 15.483 and an intercept of 0.150. Therefore, for yttrium clusters, valuable information has been achieved by the correlation between the static polarizabilities and ionization potential, which is correlated with experiment. This important observation can provide a way to calculate the polarizability of the clusters of larger size from the values of their ionization potential.

3.3.3. Softness and Hardness. For atomic systems, the softness is directly related to the polarizability. As shown in Figure 9, for the TM yttrium clusters, there also exists a linear relation between the average softness (S/n) and $\langle\alpha\rangle^{1/3}/n$. The chemical hardness per atom (η^{-1}/n) value vs the cluster size is plotted in Figure 9, which is half of the S/n value. Thus, the trends of these two parameters exhibit the same result completely. The softness, which represents essentially the charge capacity of a species, is proportional to the size for any system. On the other hand, polarizability can be approximated as R^3 (R is the radius of the sphere) for a dielectric sphere or shell, and the relation has been shown to be valid for the case of atomic systems.[94] Since the molecular systems are not spherical in general, the extension of the above relationship between the polarizability and molecular volume has not generally been successful.[22,95] However, in the present study, the above relationship is validated for TM yttrium clusters. Then strong correlations between softness and hardness and polarizability are obtained for yttrium clusters. Much further work should be done before this principle can serve as one criterion of the relation for other clusters and molecular systems.

4. Conclusions

The static dipole polarizabilities of the lowest energy structure of Y_n ($n \leq 15$) clusters have been studied within the framework of the DFT and FF methods. Electronic effects on polarizabilities with reactivity descriptors, such as the HOMO−LUMO gap, ionization energy, electron affinity, static polarizabilities, and chemical hardness and softness, have also been explored in this paper. The BP86/CEP-121G level of the DFT method is found to be reliable and therefore can be applied to predict the geometry and electronic properties for yttrium cluster. The results illuminated that the chosen theoretical method for the static dipole polarizability of yttrium clusters is reasonable at an acceptable computational level. The lowest energy structures for Y_n ($n > 3$) clusters are all found to be closed compact arrangements. Energetic analysis shows that the Y_n clusters with $n = 4$, 7, 11, and 13 are more stable than their neighboring clusters. The stability is related to the static polarizability and electronic properties for yttrium clusters, such as the mean static polarizabilities per atom, chemical hardness, and ratio of the mean static polarizability to the HOMO−LUMO gap. The static polarizability per atom decreases slowly with increasing cluster size, accompanied by some local oscillations. The ratio of the mean static polarizability to the HOMO−LUMO gap for the magic number clusters is lower than the neighboring clusters. The MPP and PMH can be used to characterize the stability of yttrium clusters, and the maximum hardness, minimum polarizability, and cluster stability complement each other. The calculated dipole moments are related to the electronic structures in which a large HOMO−LUMO gap contributes to a large dipole moment. The polarizabilities of clusters are partially related to the HOMO−LUMO gap and also dependent on the geometrical characteristics. Strongly correlated relationships between the ionization potential, softness, and cube root of polarizability are investigated for Y_n clusters. The static polarizabilities of Y_n ($n \leq 15$) clusters are clearly related to the ionization potential and increased monotonically and linearly for $\langle\alpha\rangle^{1/3}/n$ with VIP^{-1}/n and S/n, respectively.

Acknowledgment. This work is supported by the National Natural Science Foundation of China (Project Nos. 10774104 and 10804101) and the Foundation of Key Laboratory of National Defense Science and Technology of Plasma Physics, China (Project No. 9140C6805020806).

References and Notes

(1) Becker, J. A. *Angew. Chem., Int. Ed. Engl.* **1997**, *36*, 1390.

(2) Bonin, K. D.; Kresin, V. V. *Electric-Dipole Polarizabilities of Atoms, Molecules and Clusters*; World Scientific: Singapore, 1997.

(3) Kreibig, U.; Vollmer, M. *Optical Properties of Metal Clusters*; Springer: Berlin, 1995.

(4) de Heer, W. A. *Rev. Mod. Phys.* **1993**, *65*, 611.

(5) Wang, J.; Yang, M.; Wang, G.; Zhao, J. *Chem. Phys. Lett.* **2003**, *367*, 448.
(6) Deng, K.; Yang, J.; Chan, C. T. *Phys. Rev. A* **2000**, *61*, 025201.
(7) Fernández, E. M.; José, M. S.; Luis, C. B. *Phys. Rev. B* **2006**, *73*, 235433.
(8) Idrobo, J. C.; Walkosz, W.; Yip, S. F.; Öüt, S.; Wang, J.; Jellinek, J. *Phys. Rev. B* **2007**, *76*, 205422.
(9) Calaminici, P.; Köster, A. M.; Vela, A. *J. Chem. Phys.* **2000**, *113*, 2199.
(10) Yang, M.; Jackson, K. A. *J. Chem. Phys.* **2005**, *122*, 184317.
(11) Rantala, T. T.; Stockman, M. I.; Jelski, D. A.; George, T. F. *J. Chem. Phys.* **1990**, *93*, 7427.
(12) Vasiliev, I.; Öüt, S.; Chelikowsky, J. R. *Phys. Rev. Lett.* **1997**, *78*, 4805.
(13) Torrens, F. *Microelectron. Eng.* **2000**, *613*, 51–52.
(14) Torrens, F. *Nanotechnology* **2002**, *13*, 433.
(15) Fuentealba, P. *Chem. Phys. Lett.* **2004**, *397*, 459.
(16) Kłos, J. *J. Chem. Phys.* **2005**, *123*, 024308.
(17) Chu, X.; Dalgarno, A.; Groenenboom, G. C. *Phys. Rev. A* **2005**, *72*, 032703.
(18) Papadopoulos, M. G.; Reis, H.; Avramopoulos, A.; Erkoç, S.; Amirouche, L. *J. Phys. Chem. B* **2005**, *109*, 18822.
(19) Fuentealba, P.; Simon, Y. *J. Phys. Chem.* **1997**, *101*, 4231.
(20) Fuentealba, P. *Phys. Rev. A* **1998**, *58*, 4232.
(21) Jaque, P.; Toro-Labbé, A. *J. Chem. Phys.* **2002**, *117*, 3208.
(22) Chandrakumar, K. R. S.; Ghanty, T. K.; Ghosh, S. K. *J. Chem. Phys.* **2004**, *120*, 6487.
(23) Calaminici, P. *Chem. Phys. Lett.* **2004**, *387*, 253.
(24) Idrobo, J. C.; Öüt, S.; Jellinek, J. *Phys. Rev. B* **2005**, *72*, 085445.
(25) Yang, M.; Jackson, K. A.; Jellinek, J. *J. Chem. Phys.* **2006**, *125*, 144308.
(26) Wang, J.; Yang, M.; Jellinek, J.; Wang, G. *Phys. Rev. A* **2006**, *74*, 023202.
(27) Chandrakumar, K. R. S.; Ghanty, T. K.; Ghosh, S. K. *J. Phys. Chem. A* **2004**, *108*, 6661.
(28) Rayane, D.; Allouche, A. R.; Benichou, E.; Antoine, R.; Aubert-Frecon, M.; Dugourd, Ph.; Broyer, M.; Ristori, C.; Chandezon, F.; Huber, B. A.; Guet, C. *Eur. Phys. J. D* **1999**, *9*, 243.
(29) Knickelbein, M. B. *J. Chem. Phys.* **2001**, *115*, 5957.
(30) Knickelbein, M. B. *J. Chem. Phys.* **2003**, *118*, 6230.
(31) Moro, R.; Xu, X.; Yin, S.; de Heer, W. A. *Science* **2003**, *300*, 1265.
(32) Knickelbein, M. B. *J. Chem. Phys.* **2004**, *120*, 10450.
(33) Fedrigo, S.; Harbich, W.; Belyaev, J.; Buttet, J. *Chem. Phys. Lett.* **1993**, *211*, 166.
(34) Knight, W. D.; Clemenger, K.; de Heer, W. A.; Saunders, W. A. *Phys. Rev. B* **1985**, *31*, 2539.
(35) Benichou, E.; Antoine, R.; Rayane, D.; Vezin, B.; Dalby, F. W.; Dugourd, Ph.; Broyer, M.; Ristori, C.; Chandezon, F.; Huber, B. A.; Rocco, J. C.; Blundell, S. A.; Guet, C. *Phys. Rev. A* **1999**, *59*, R1.
(36) Antoine, R.; Rayane, D.; Allouche, A. R.; Aubert-Fre'con, M.; Benichou, E.; Dalby, F. W.; Dugourd, Ph.; Broyer, M.; Guet, C. *J. Chem. Phys.* **1999**, *110*, 5568.
(37) Dmitrieva, I. K.; Plindov, G. I. *Phys. Scr.* **1983**, *27*, 402.
(38) Knickekbein, M. *J. Chem. Phys.* **1995**, *102*, 1.
(39) Pearson, R. G. *Chemical Hardness: Applications from Molecules to Solids*; Wiley-VCH Verlag GMBH: Weinheim, Germany, 1997.
(40) Ghanty, T. K.; Ghosh, S. K. *J. Phys. Chem.* **1996**, *100*, 17429.
(41) Poltizer, P.; Grice, M. D.; Murray, J. S. *J. Mol. Struct.: THEOCHEM* **2001**, *549*, 69.
(42) Chandrakumar, K. R. S.; Ghanty, T. K.; Ghosh, S. K. *J. Phys. Chem. A* **2004**, *108*, 6661.
(43) Knight, L. B., Jr.; Woodward, R. W.; Van Zee, R. J.; Weltner, W. *J. Chem. Phys.* **1983**, *79*, 5820.
(44) Morse, M. D. *Chem. Rev.* **1986**, *86*, 1049.
(45) Dai, D.; Balasubramanian, K. *J. Chem. Phys.* **1993**, *98*, 7098.
(46) Wu, Z. J.; Zhang, H. J.; Meng, J.; Dai, Z. W.; Han, B.; Jin, P. C. *J. Chem. Phys.* **2004**, *121*, 4699.
(47) Wu, Z. J. *Chem. Phys. Lett.* **2004**, *383*, 251.
(48) Yuan, H. K.; Chen, H.; Kuang, A. L.; Ahmed, A. S.; Xiong, Z. H. *Phys. Rev. B* **2007**, *75*, 174412.
(49) Dai, D.; Balasubramanian, K. *Chem. Phys. Lett.* **1995**, *238*, 203.
(50) Durakiewicz, T.; Halas, S. *Chem. Phys. Lett.* **2001**, *341*, 195.
(51) Mao, H. P.; Yang, L. R.; Wang, H. Y.; Zhu, Z. H.; Tang, Y. J. *Acta Phys. Sin.* **2005**, *54*, 5126.
(52) Li, X. B.; Wang, H. Y.; Yang, X. D.; Zhu, Z. H.; Tang, Y. J. *J. Chem. Phys.* **2007**, *126*, 084505.
(53) Wang, H. Y.; Li, X. B.; Tang, Y. J.; Mao, H. P.; Zhu, Z. H. *Chin. J. Chem. Phys.* **2005**, *18*, 50.
(54) Rubio, A.; Balbás, L. C.; Serra, L1.; Barranco, M. *Phys. Rev. B* **1990**, *42*, 10950.
(55) Matsuzawa, N.; Seto, J.; Dixon, D. A. *J. Phys. Chem. A* **1997**, *101*, 9391.
(56) Perpete, E. A.; Champagne, B.; Kirtman, B. *Phys. Rev. B* **2000**, *61*, 13137.
(57) Li, X. B.; Luo, J. S.; Guo, Y. D.; Wu, W. D.; Wang, H. Y.; Tang, Y. J. *Acta Phys. Sin.* **2008**, *57*, 4857.
(58) Perdew, J. P. *Phys. Rev. B* **1986**, *33*, 8822.
(59) Becke, A. D. *Phys. Rev. A* **1988**, *38*, 3098.
(60) Krauss, M.; Stevens, W. J. *Annu. Rev. Phys. Chem.* **1984**, *35*, 357.
(61) Han, J. G.; Sheng, L. S.; Zhang, Y. W.; Morales, J. A. *Chem. Phys.* **2003**, *249*, 211.
(62) Jansik, B.; Schimmelpfennig, B.; Norman, P.; Mochizuki, Y.; Luo, Y.; Ågren, H. *J. Phys. Chem. A* **2002**, *106*, 395.
(63) Wang, J.; Han, J. G. *J. Chem. Phys.* **2005**, *123*, 244303.
(64) Stevens, W. J.; Krauss, M.; Basch, H. *Can. J. Chem.* **1992**, *70*, 612.
(65) Walch, S. P. *Theor. Chim. Acta* **1987**, *71*, 449.
(66) Bauschlicher, C. W., Jr.; Langhoff, S. R.; Partridge, H. *Phys. Chem.* **1990**, *94*, 8378.
(67) Verhaegen, G. *J. Chem. Phys.* **1964**, *40*, 239.
(68) Fang, L.; Chen, X.; Shen, X.; Liu, Y.; Lindsay, D. M.; Lombardi, J. R. *Low Temp. Phys.* **2000**, *26*, 752.
(69) Jules, J. L.; Lombardi, J. R. *J. Phys. Chem. A* **2003**, *107*, 1268.
(70) Kurtz, H. A.; Stewart, J. J. P.; Dieter, K. M. *J. Comput. Chem.* **1990**, *11*, 82.
(71) Frisch, M. J.; Trucks, G. W.; Schlegel, H. B.; Scuseria, G. E.; Robb, M. A.; Cheeseman, J. R.; Montgomery, J. A., Jr.; Vreven, T.; Kudin, K. N.; Burant, J. C.; Millam, J. M.; Iyengar, S. S.; Tomasi, J.; Barone, V.; Mennucci, B.; Cossi, M.; Scalmani, G.; Rega, N.; Petersson, G. A.; Nakatsuji, H.; Hada, M.; Ehara, M.; Toyota, K.; Fukuda, R.; Hasegawa, J.; Ishida, M.; Nakajima, T.; Honda, Y.; Kitao, O.; Nakai, H.; Klene, M.; Li, X.; Knox, J. E.; Hratchian, H. P.; Cross, J. B.; Bakken, V.; Adamo, C.; Jaramillo, J.; Gomperts, R.; Stratmann, R. E.; Yazyev, O.; Austin, A. J.; Cammi, R.; Pomelli, C.; Ochterski, J. W.; Ayala, P. Y.; Morokuma, K.; Voth, G. A.; Salvador, P.; Dannenberg, J. J.; Zakrzewski, V. G.; Dapprich, S.; Daniels, A. D.; Strain, M. C.; Farkas, O.; Malick, D. K.; Rabuck, A. D.; Raghavachari, K.; Foresman, J. B.; Ortiz, J. V.; Cui, Q.; Baboul, A. G.; Clifford, S.; Cioslowski, J.; Stefanov, B. B.; Liu, G.; Liashenko, A.; Piskorz, P.; Komaromi, I.; Martin, R. L.; Fox, D. J.; Keith, T.; Al-Laham, M. A.; Peng, C. Y.; Nanayakkara, A.; Challacombe, M.; Gill, P. M. W.; Johnson, B.; Chen, W.; Wong, M. W.; Gonzalez, C.; Pople, J. A. *Gaussian 03*, revision C.3; Gaussian, Inc.: Pittsburgh, PA, 2003.
(72) Parr, R. G.; Yang, W. *Density Functional Theory of Atoms and Molecules*; Oxford University Press: New York, 1989.
(73) Parr, R. G.; Donnelly, R. A.; Levy, M.; Palke, W. E. *J. Chem. Phys.* **1978**, *68*, 3801.
(74) Parr, R. G.; Pearson, R. G. *J. Am. Chem. Soc.* **1983**, *105*, 7512.
(75) Pearson, R. G. *J. Am. Chem. Soc.* **1985**, *107*, 6801.
(76) Pearson, R. G.; Palke, W. E. *J. Phys. Chem.* **1992**, *96*, 3283.
(77) Ghanty, T. K.; Ghosh, S. K. *J. Phys. Chem.* **1993**, *97*, 4951.
(78) Sen, K. D. *Structure and Bonding: Chemical Hardness*; Springer-Verlag: Berlin, 1993.
(79) Chattaraj, P. K.; Liu, G. H.; Parr, R. G. *Chem. Phys. Lett.* **1995**, *237*, 171.
(80) Pearson, R. G. *Inorg. Chem.* **1984**, *23*, 4675.
(81) Pearson, R. G. *J. Am. Chem. Soc.* **1988**, *110*, 7684.
(82) Pérez, P.; Toro-Labbé, A. *Theor. Chem. Acc.* **2001**, *105*, 422.
(83) Jaque, P.; Toro-Labbé, A. *J. Phys. Chem. A* **2000**, *104*, 995.
(84) Gutiérrez-Oliva, S.; Jaque, P.; Toro-Labbé, A. *J. Phys. Chem. A* **2000**, *104*, 8955.
(85) Pérez, P.; Toro-Labbé, A. *J. Phys. Chem. A* **2000**, *104*, 1557.
(86) Torrent-Sucarrat, M.; Luis, J. M.; Duran, M.; Solà, M. *J. Am. Chem. Soc.* **2001**, *103*, 7951.
(87) Yang, Z.; Xiong, S. J. *J. Chem. Phys.* **2008**, *129*, 124308.
(88) Chu, X.; Dalgarno, A.; Groenenboom, G. C. *Phys. Rev. A* **2007**, *75*, 032723.
(89) Chattaraj, P. K.; Sengupta, S. *J. Phys. Chem.* **1996**, *100*, 16126.
(90) Chattaraj, P. K.; Poddar, A. *J. Phys. Chem. A* **1998**, *102*, 9944.
(91) Chattaraj, P. K.; Fuentealba, P.; Jaque, P.; Toro-Labbé, A. *J. Phys. Chem. A* **1999**, *103*, 9307.
(92) Orr, B. J.; Ward, J. F. *Mol. Phys.* **1971**, *20*, 513.
(93) Oudar, J. L. *J. Chem. Phys.* **1977**, *67*, 446.
(94) Politzer, P.; Jim, P.; Murray, J. S. *J. Chem. Phys.* **2002**, *117*, 8197.
(95) Brinck, T.; Murray, J. S.; Politzer, P. *J. Chem. Phys.* **1993**, *98*, 4305.
(96) Ghanty, T. K.; Ghosh, S. K. *J. Phys. Chem.* **1996**, *100*, 12295.
(97) Ghanty, T. K.; Ghosh, S. K. *J. Phys. Chem.* **2000**, *104*, 2975.
(98) Hellmann, H. *Einführung in die Quantenchemie*, Deuticke: Leipzig, Germany, 1937; p 285.
(99) Feynman, R. P. *Phys. Rev.* **1939**, *56*, 340.
(100) Hush, N. S.; Williams, M. L. *Chem. Phys. Lett.* **1970**, *5*, 507.
(101) Hush, N. S.; Williams, M. L. *Chem. Phys. Lett.* **1970**, *6*, 63.
(102) Gready, J. E.; Bacskay, G. B.; Hush, N. S. *Chem. Phys.* **1977**, *24*, 333.
(103) Metzger, R. M. *Chem. Phys.* **2006**, *326*, 176.

JP904420Z